Proton-helium collisions at intermediate energies: Singly differential ionization cross sections

K. H. Spicer,[1,*] C. T. Plowman,[1] I. B. Abdurakhmanov,[1] Sh. U. Alladustov,[2] I. Bray,[1] and A. S. Kadyrov[1,†]

[1]*Curtin Institute for Computation and Department of Physics and Astronomy, Curtin University, GPO Box U1987, Perth, Western Australia 6845, Australia*

[2]*Uzbek-Israel Joint Faculty, National University of Uzbekistan, Tashkent, 100174, Uzbekistan*

(Received 28 September 2021; accepted 12 November 2021; published 24 November 2021)

We investigate the four-body proton-helium scattering problem using the two-center wave-packet convergent close-coupling approach. The approach uses a correlated two-electron wave function for the helium target. The continuum is discretized using wave-packet pseudostates. Calculations of ionization cross sections differential in the electron emission energy, in the emission angle, as well as in the scattered-projectile angle are performed in the intermediate energy region where coupling between various channels and electron-electron correlation effects are important. The results agree well with experimental data, where available. Moreover, our calculations reveal an interesting interplay between direct ionization and electron capture into the continuum. In particular, we demonstrate that the ionization cross section differential in the angle of the ejected electron is dominated by electron capture into the continuum for ejection into small angles, while ejection into large angles is purely due to direct ionization. It is concluded that the two-center wave-packet convergent close-coupling approach can provide accurate singly differential cross sections for ionization in proton-helium collisions. For comparison, a recently developed method that reduces the target to an effective single-electron system is also used. Somewhat unexpectedly, the results of the effective one-electron method exhibit a very good level of agreement with the full two-electron ones for all three singly differential cross sections. Therefore, we also conclude that, at least for the purpose of calculating the singly differential cross sections for single ionization of helium, an effective one-electron treatment of the target suffices.

DOI: 10.1103/PhysRevA.104.052815

I. INTRODUCTION

The study of ion-atom collisions has been, and still is, one of the intensive areas of research within atomic physics. A complete understanding of the processes of excitation, ionization, and charge exchange occurring in collisions is essential for applications in areas such as astrophysics and plasma physics. Such collisional phenomena are also relevant to hadron therapy. Many approaches to modeling atomic collisions have been developed [1–3]. For a recent review of energetic ion-atom and ion-molecule collisions, see Ref. [4].

The simplest four-body scattering problem is presented by collisions of protons with helium atoms. Solving this problem in full remains challenging. While investigations into the particular processes of electron capture, elastic scattering, and target excitation have progressed, few attempts have been made to probe the ionization process in a nonperturbative manner [5,6]. We consider the intermediate energy region where the projectile speed is either comparable to, or somewhat larger than, the electron's orbital speed. At these energies, coupling between various channels cannot be ignored. The difficulty in modeling ionization comes from the fact that, in the exit channel, the ejected electron moves in the Coulombic field of both the target nucleus and the projectile. When the projectile ionizes the atom, it may do so through either direct ionization (DI), or electron capture to the continuum (ECC). This then requires that two-center effects be accounted for in any theoretical calculation of ionization cross sections. Furthermore, another possible higher-order effect has been suggested to hold even greater importance upon the recent collection of fully differential cross-section data for the proton-helium collision system at the intermediate projectile impact-energy of 75 keV by Schulz *et al.* [7]. Peak structures present in the forward-scattering direction and in the perpendicular-scattering plane indicate that some intricate two-electron mechanisms might be influencing the single-electron ionization process. Furthermore, theory fails when it comes to measurements of two-electron processes like transfer excitation [8,9]. This indicates that the full proton-helium problem is far from being solved.

The proton-impact ionization of helium has been investigated experimentally [10–21] and theoretically [11,12,16,22–35] to obtain total and singly differential cross sections. In this work we focus our attention on the singly differential cross sections, which provide a more detailed differential picture of ionization. Since ionization is a challenging process to model, the majority of theoretical approaches are based on the first-order Born approximation (FBA) [15,18,20–22,24,28,30,34]. These approaches employ different initial-state wave functions. In particular, the scaled hydrogen-like

*kate.bain@graduate.curtin.edu.au
†a.kadyrov@curtin.edu.au

[20,30], Hartree-Fock [18], and Hartree-Slater [15,34] wave functions are used to describe the target ground state in the initial channel. The plane-wave first-order Born approximation (PWBA) uses the plane wave to describe the relative motion of the heavy particles. It can, e.g., be done either in the Born approximation excluding or including the postcollision interaction (PCI) [21]. These two particular approaches are referred to hereafter as BA and BA-PCI, respectively. The theoretical approaches based on the FBA have typically produced good agreement for total ionization cross sections at high energies but close quantitative agreement in differential ionization has been weak, particularly for angular distributions. The results of the FBA for cross sections differential in ejected-electron energy and angle using the Hartree-Fock and Hartree-Slater wave function for the target describe the experimental data [17,18,20] better than the hydrogen-like FBA, as expected. In the case of cross sections's differential in the projectile scattering angle, the results of the FBA using Hartree-Slater wave functions [34] were in fair agreement with the experimental data at 300 keV [13], but those of the PWBA [24] found agreement only in the narrow forward-scattering region. For energy-differential cross sections, the BA results at 75 and 150 keV showed good agreement with the experiment. The BA-PCI results at 75 keV were scaled by a factor of 0.5 to compare with the experimental data, leading to good agreement in shape [21]. Fair agreement between the BA-PCI calculations and the experimental data of Schulz *et al.* [21] was found at 100 and 150 keV. The first Born approximation, when applied to the calculation of ionization cross section as a function of ejected-electron angle, led to fair agreement with experimental data [15,20]. Finally, the Bethe expansion [28] took the FBA and expanded it in inverse powers of $T = mv^2/2$ where m is the electron mass and v is the projectile velocity. This model provided fairly accurate differential cross sections for both 100 and 300 keV projectile-impact energies in the mrad scattering angle range presented.

Other perturbative methods are the continuum distorted-wave (CDW) method of Barna *et al.* [22], continuum-distorted-wave eikonal-initial-state (CDW-EIS) approaches of Bernardi *et al.* [11] and Barna *et al.* [22], and the eikonal distorted-wave approach of Fukuda *et al.* [24]. For ionization as a function of the ejected-electron angle, there is fair agreement between the CDW-EIS approach and experiment of Bernardi *et al.* [11] at a proton-impact energy of 100 keV. For 300 keV, the CDW and CDW-EIS approaches [22] also achieved adequate agreement, particularly with the experiments of Toburen [15] and Stolterfoht [20], across the entire angular range. Similar agreement was found for cross sections as a function of the projectile-scattering angle in the case of the eikonal distorted-wave method using a static potential [24] when compared with the experiment of Giese and Horsdal [13]. A Coulomb potential was also used by Fukuda *et al.* [24], though the results obtained tended to overestimate the experimental data in the intermediate angle region.

Classical-trajectory Monte Carlo (CTMC) calculations of Reinhold and Falcón [32] and Reinhold and Olson [33] agree fairly well with experimental data for the ejected-electron energy distribution [17,18,20,21], though slightly underestimate them at larger electron energies. The approach is in agreement with the experiment of Gibson and Reid [12] at 100 keV on ejected-electron angular differential cross sections, which falls below the experiments of Rudd and Madison [18], Rudd and Jorgensen [17], and Rudd *et al.* [20] at angles greater than 60°. The calculation of Barna *et al.* [22] has a similar shape to the corresponding calculation of Gibson and Reid [12], underestimating experimental data [15,20] for large scattering angles. For the cross sections's differential in the projectile-scattering angle, Meng *et al.* [16] employed the dynamical CTMC (dCTMC) with agreement for larger angles of the mrad range presented but underestimates the experiment at 300 keV [13] for angles near 0. Schultz and Olson [35] applied the CTMC approach at 100 keV, though no experimental data was available for comparison.

A binary-encounter method employing the virial-theorem by Garcia [36] and a binary-encounter free-fall (BE-FF) method by Gryziński [25,26] were applied to the calculation of singly differential cross sections's differential in ejected-electron energy. These classical approaches produced results that were found to be in adequate agreement with the experimental data for 100 keV [17,18,20,21] and agreed well with data at 300 keV [20]. Another approach, the classical impulse approximation by Bell *et al.* [23], also produced results in fairly good agreement with experimental data by Rudd *et al.* [20] at both 100 and 300 keV.

The brief overview given above shows that the close-coupling formalism has rarely been applied to differential ionization in proton-helium collisions. The close-coupling approaches have certain challenges. In the high-energy regime, the interaction matrix elements become highly oscillatory, making numerical evaluations extremely challenging. This makes reaching convergence in terms of the number of the included basis states a difficult task. There are also challenges with modeling the continuum, restricting the applicability of the close-coupling methods, particularly in the energy range considered herein where the probability of capture into the continuum of the projectile cannot be ignored. The authors are aware of only one attempt at applying a close-coupling formulation to differential ionization in proton-helium collisions, the single-center coupled-channel (CC) approach of Barna *et al.* [22] which was used to calculate the ionization cross section as a function of ejected-electron angle. Agreement with the experiments of Rudd *et al.* [20], Toburen [15], and Stolterfoht [20] was somewhat poor. The convergent close-coupling approach has been developed to circumvent the aforementioned difficulties through use of the fully quantum-mechanical [37,38], standard semiclassical [39], and wave-packet [40,41] implementations for the fundamental proton-hydrogen collision system. The wave-packet convergent close-coupling (WP-CCC) method was most recently applied to the calculation of singly differential cross sections for the proton-hydrogen system [42], leading to excellent agreement with the experiment. The method was also extended to the proton-helium differential ionization [43,44] at sufficiently high energies where electron capture channels can be neglected. Also note that the integrated cross sections were calculated using the two-center WP-CCC approach and the obtained results agree very well with the experiment in a wide energy range including low, intermediate, and high energies [6].

Some approaches to proton-helium scattering give very good results for particular reaction channels, like electron capture, however, they cannot provide information on other concurrent channels. There has been no attempt to calculate all the interconnected processes on equal footing at the same time and in a systematic fashion. Our aim here is to fill in this gap. Thus far, calculations of the differential cross sections for electron capture, elastic scattering, and target excitation have been completed and reported in Ref. [45] (hereafter referred to as Paper I). It was concluded that the WP-CCC approach was capable of providing a complete and reasonably accurate differential picture of the binary processes taking place in proton-helium collisions. In this work, the two-center four-body semiclassical WP-CCC method is used to calculate cross sections for ionization in proton-helium collisions singly differential in the ejected electron energy, in the electron emission angle, and in the scattered-projectile angle at the same four intermediate incident-projectile energies as in Paper I. For comparison, we also use a recently developed approach [46] that reduces the two-electron helium atom to an effective single-electron system convenient for scattering calculations. Here we report the results obtained using both methods.

Unless specified otherwise, atomic units (a.u.) are used throughout this paper.

II. TWO-CENTER WAVE-PACKET CONVERGENT CLOSE-COUPLING METHOD

A. Scattering equations

Various aspects of the two-center wave-packet-convergent close-coupling method for ion-atom collisions are described in detail in our earlier works [6,41,43,47,48]. The approach has been extended to multicharged projectiles in Refs. [49,50] and to two-electron targets in Ref. [6]. Furthermore, the one-center WP-CCC approach to two-center rearrangement collisions was developed by the authors of Ref. [51]. A brief description of the two-center method is given here with emphasis on the parts relevant to the present calculations.

We apply the frozen-core approximation for the helium atom and the semiclassical approximation for the collision system, which are valid in the energy region where we perform our present calculations. The exact nonrelativistic time-independent Schrödinger equation for the total scattering wave function Ψ is

$$(H - E)\Psi = 0, \tag{1}$$

where H is the full four-body Hamiltonian and E is the total energy of the collision system. We assume that the target nucleus is located at the origin and the projectile is moving along the trajectory $\boldsymbol{R} \equiv \boldsymbol{R}(t) = \boldsymbol{b} + \boldsymbol{v}t$, where $\boldsymbol{b}$ is the impact parameter and $\boldsymbol{v}$ is the initial velocity of the projectile relative to the target. The impact parameter vector is perpendicular to the velocity vector, such that $\boldsymbol{b} \cdot \boldsymbol{v} = 0$. Then assuming the total electronic spin of helium is conserved throughout the collision, the total scattering wave function for the correlated two-electron helium target is expanded in terms of N target-centered and M projectile-centered pseudostates as

$$\begin{aligned}\Psi = &\sum_{\alpha=1}^{N} a_\alpha \psi_\alpha^{\mathrm{He}}(\boldsymbol{r}_1, \boldsymbol{r}_2) e^{i\boldsymbol{k}_\alpha \boldsymbol{\sigma}} \\ &+ \frac{1}{\sqrt{2}} \sum_{\beta=1}^{M} b_\beta \big[\psi_\beta^{\mathrm{H}}(\boldsymbol{x}_1)\psi_{1s}^{\mathrm{He}^+}(\boldsymbol{r}_2) e^{i\boldsymbol{k}_{1\beta}\boldsymbol{\rho}_1} \\ &+ \psi_\beta^{\mathrm{H}}(\boldsymbol{x}_2)\psi_{1s}^{\mathrm{He}^+}(\boldsymbol{r}_1) e^{i\boldsymbol{k}_{2\beta}\boldsymbol{\rho}_2}\big],\end{aligned} \tag{2}$$

where the indices α and β denote the full set of quantum numbers that represent, respectively, a quantum state in the p-He channel and the H-He^+ rearrangement channel, formed after electron capture by the projectile. The position vectors of the two electrons relative to the helium nucleus are $\boldsymbol{r}_1$ and $\boldsymbol{r}_2$, respectively, and the position vectors of the electrons relative to the incident proton are $\boldsymbol{x}_1$ and $\boldsymbol{x}_2$. The position vector of the proton relative to the center of mass of the helium atom is $\boldsymbol{\sigma}$ and the position vector of the proton and first (second) electron system relative to the helium ion is $\boldsymbol{\rho}_1$ ($\boldsymbol{\rho}_2$). Accordingly, $\boldsymbol{k}_\alpha$ is the momentum of the projectile relative to the helium atom in the α channel. Similarly, $\boldsymbol{k}_{1\beta}$ ($\boldsymbol{k}_{2\beta}$) is the momentum of the hydrogen atom relative to the residual helium ion in the 1β (2β) channel. Channels 1β and 2β are the same, but have the electron of the hydrogen atom and the electron of the residual helium ion exchanged. Thus, our method accounts for the exchange effects between the captured electron and the electron of the residual He^+ ion. In the above equation, $\psi_\alpha^{\mathrm{He}}$ and ψ_β^{H} are the wave functions of the helium and hydrogen atoms, respectively, and $\psi_{1s}^{\mathrm{He}^+}$ is the ground-state wave function for the helium ion. The expansion coefficients a_α and b_β, which are functions of $\boldsymbol{\sigma}$ and $\boldsymbol{\rho}$, represent the transition amplitudes into the corresponding final channel as $\sigma, \rho \to +\infty$. By substituting the expansion in Eq. (2) into Eq. (1) we obtain a set of coupled first-order differential equations for the expansion coefficients. See Paper I and Ref. [6] for details.

In this work we calculate all three possible singly differential cross sections (SDCS) for ionization. The ionization cross sections differential in the energy and in the angle of the ejected electron can be calculated from the fully differential cross section, respectively, as

$$\frac{d\sigma_{\mathrm{ion}}}{dE_e} = \int \frac{d^3\sigma_{\mathrm{ion}}}{dE_e d\Omega_e d\Omega_f} d\Omega_f d\Omega_e, \tag{3}$$

and

$$\frac{d\sigma_{\mathrm{ion}}}{d\Omega_e} = \int \frac{d^3\sigma_{\mathrm{ion}}}{dE_e d\Omega_e d\Omega_f} d\Omega_f dE_e, \tag{4}$$

where Ω_e is the solid angle of $\boldsymbol{\kappa}$, the electron momentum in the laboratory frame, into which the electron is ejected, $E_e(=\kappa^2/2)$ is the ejected electron energy, and Ω_f is the solid angle of the scattered projectile. The ionization cross section differential in the angle of the scattered projectile can be calculated as

$$\frac{d\sigma_{\mathrm{ion}}}{d\Omega_f} = \int \frac{d^3\sigma_{\mathrm{ion}}}{dE_e d\Omega_e d\Omega_f} d\Omega_e dE_e. \tag{5}$$

In the current two-center approach, the fully differential cross section for ionization consists of the incoherent

combination of the direct ionization and electron-capture into continuum components. In the laboratory frame it is written as

$$\frac{d^3\sigma_{\rm ion}}{dE_e d\Omega_e d\Omega_f} = \frac{\mu_T^2}{(2\pi)^2}\frac{q_f \kappa}{q_i}\left(\left|T_{fi}^{\rm DI}(\boldsymbol{\kappa}, \boldsymbol{q}_f, \boldsymbol{q}_i)\right|^2 + \left|T_{fi}^{\rm ECC}(\boldsymbol{\kappa} - \boldsymbol{v}, \boldsymbol{q}_f, \boldsymbol{q}_i)\right|^2\right), \quad (6)$$

where, as mentioned above, Ω_f is the solid angle of $\boldsymbol{q}_f$ (relative to $\boldsymbol{q}_i$). We choose the target to be in its ground state in the initial channel. Therefore, we set $\boldsymbol{q}_i = \boldsymbol{k}_1$ in both terms, however, $\boldsymbol{q}_f = \boldsymbol{k}_{\alpha'}$ in the DI term and $\boldsymbol{q}_f = \boldsymbol{k}_{1\beta'} \equiv \boldsymbol{k}_{2\beta'}$ in the ECC term. The reduced mass in the p-He channel is denoted as μ_T. As discussed below, the ionization amplitudes $T_{fi}^{\rm DI}(\boldsymbol{\kappa}, \boldsymbol{q}_f, \boldsymbol{q}_i)$ and $T_{fi}^{\rm ECC}(\boldsymbol{\kappa} - \boldsymbol{v}, \boldsymbol{q}_f, \boldsymbol{q}_i)$ are expressed in terms of the time-dependent coefficients a_f and b_f in the asymptotic region.[1]

According to the idea developed in Ref. [54], the ionization amplitude can be found by projecting the positive-energy pseudostates on both centers onto the true Coulomb scattering wave function. It is based on the surface-integral formulation of scattering theory [55,56] that gives a definition of the Coulomb breakup amplitude in the postform. Full details of the WP-CCC approach to differential ionization are given in Ref. [41] for proton-impact ionization of hydrogen. Generalizing this approach to the proton-impact ionization of helium, we can write the amplitude for direct ionization of the target atom in terms of the direct-scattering (DS) amplitude as

$$T_{fi}^{\rm DI}(\boldsymbol{\kappa}, \boldsymbol{q}_f, \boldsymbol{q}_i) = \langle \varphi_{\boldsymbol{\kappa}}^{\rm He} | \psi_f \rangle T_{fi}^{\rm DS}(\boldsymbol{q}_f, \boldsymbol{q}_i), \quad (7)$$

where $\varphi_{\boldsymbol{\kappa}}^{\rm He}$ is the wave function representing the true continuum state of the ejected electron with momentum $\boldsymbol{\kappa}$ relative to the target residual He^+ ion. This wave function is obtained by numerically solving the Schrödinger equation (either full two-electron or effective one-electron, depending on the method used) for the He atom. Thus, we see that the DI amplitude is given in terms of the amplitude for excitation of the corresponding positive-energy pseudostate. The amplitude for electron capture into the continuum of the atom formed by the projectile can be written in terms of the electron-capture (EC) amplitude as

$$T_{fi}^{\rm ECC}(\boldsymbol{\varkappa}, \boldsymbol{q}_f, \boldsymbol{q}_i) = \langle \varphi_{\boldsymbol{\varkappa}}^{\rm H} | \psi_f \rangle T_{fi}^{\rm EC}(\boldsymbol{q}_f, \boldsymbol{q}_i), \quad (8)$$

where $\varphi_{\boldsymbol{\varkappa}}^{\rm H}$ is the true Coulomb wave representing the continuum state of the ejected electron with momentum $\boldsymbol{\varkappa}$ relative to the projectile nucleus. Thus, the ECC amplitude is given in terms of the amplitude for electron capture into the corresponding positive-energy pseudostate.

The direct scattering amplitudes $T_{fi}^{\rm DS}$ and electron-capture amplitudes $T_{fi}^{\rm EC}$ are calculated from the impact-parameter space transition probability amplitudes as follows:

$$T_{fi}^{\rm DS}(\boldsymbol{q}_f, \boldsymbol{q}_i) = 2\pi i v e^{im\phi_f} \int_0^\infty dbb[\tilde{a}_f(+\infty, b) - \delta_{fi}] J_m(q_\perp b), \quad (9)$$

and

$$T_{fi}^{\rm EC}(\boldsymbol{q}_f, \boldsymbol{q}_i) = 2\pi i v e^{im\phi_f} \int_0^\infty dbb\tilde{b}_f(+\infty, b) J_m(q_\perp b), \quad (10)$$

where $q_\perp$ is the magnitude of the perpendicular component of the momentum transfer $\boldsymbol{q} = \boldsymbol{q}_i - \boldsymbol{q}_f$, m is the magnetic quantum number of the bound state in the final channel, ϕ_f is the azimuthal angle of $\boldsymbol{q}_f$, and J_m is the Bessel function of the mth order. For details of the above procedures we refer to Sec. 3.8 of Ref. [1]. The probability amplitudes are related to the expansion coefficient as

$$\tilde{a}_f(t, b) = e^{im\phi_{\boldsymbol{b}}} a_f(t, \boldsymbol{b}), \quad (11)$$

and

$$\tilde{b}_f(t, b) = e^{im\phi_{\boldsymbol{b}}} b_f(t, \boldsymbol{b}), \quad (12)$$

where $\phi_{\boldsymbol{b}}$ is the azimuthal angle of $\boldsymbol{b}$. For convenience, the expansion coefficients are expressed as $a_\alpha(t, \boldsymbol{b})$ and $b_\beta(t, \boldsymbol{b})$ to be functions of time and impact parameter. For further details of the direct-scattering and electron-capture amplitudes, see Paper I and Ref. [6].

B. Effective single-electron treatment of the helium target

A proper treatment of bare-ion collisions with multielectron targets is very involved theoretically and time-consuming computationally. On the other hand, there are no such structure-related complications in the case of bare-ion collisions with a hydrogen-like system. Therefore, for comparison, we also perform calculations using a recently developed method [46] that allows one to reduce the multielectron target to an effective single-electron system. Then we can take advantage of our existing numerical methods that have been implemented for bare-ion collisions with one-electron targets and reduce the amount of required computational resources when calculating cross sections.

Below we briefly summarize the effective single-electron (E1E) technique as applied to the helium target. First we use a computational atomic-structure package based on the multiconfiguration Hartree-Fock approach to produce an accurate two-electron wave function for the ground state of helium. Using the obtained ground-state wave function we calculate the probability density for the entire atom. We then average this density function over the spatial coordinates and spin variables of both target electrons, except for the distance of any one electron from the nucleus, resulting in a single-electron density function representing the probability of finding one electron of the target at a certain distance from the target nucleus. For the ground state, this function is generally nodeless, and therefore, its positive (or, equivalently, negative) square root defines the corresponding single-electron wave

[1] In previous literature the term ECC was used to denote one specific mechanism where the velocity of the ejected electron and that of the scattered projectile coincide resulting in a peak in the doubly differential ionization cross section, see, e.g., Refs. [52,53]. In this work, we use the term more broadly to describe electron transfer into all projectile continuum states. Thus, according to the convention adopted here, the narrow definition of the ECC corresponds to one point where the extended definition of the ECC reaches its maximum. Our approach demonstrates that geometries and kinematical regimes surrounding the peak also contribute to electron capture to the continuum.

function. Inserting the ground state wave function into the two-electron Schrödinger equation for the target leads to an effective single-electron equation and allows us to calculate a pseudopotential representing the collective field produced by the target nucleus and the other target electron. Our pseudopotential produces results in excellent agreement with those obtained in similar studies [57,58]. With the known ground-state radial wave function, the pseudopotential can be found by inversely solving the reduced Schrödinger equation which is then used to find radial wave functions for the excited bound states and the continuum state of the active electron. Next, the wave-packet pseudostates are constructed following the wave-packet continuum discretization approach. Obtained radial functions of the ground and a sufficient number of excited states together with the wave-packet pseudostates form a basis which describes the two-electron target. See Ref. [46] for further details.

III. CALCULATIONS OF SINGLY DIFFERENTIAL CROSS SECTIONS FOR IONIZATION

Below we present the results obtained for the all three possible singly differential cross sections for ionization at four intermediate incident-projectile energies: 75, 100, 150, and 300 keV. These are the same energies as used in Paper I, where the results on the differential cross-section calculations of the concurrent binary processes were reported. As in Paper I, our main results obtained using the correlated two-electron wave-packet convergent close-coupling approach are denoted as WP-CCC. For comparison, we also present results obtained using the effective one-electron treatment of the helium target described in Sec. II B. In both approaches the number of included negative- and positive-energy pseudostates are increased until adequate convergence is achieved in the predicted cross sections for the collision process that we are interested in. Further details of the calculations are described in Paper I. It goes without saying that the integration of each of the three singly differential cross sections reproduces the total ionization cross section obtained by summing the cross sections for excitation of the positive-energy WP pseudostates. The deviation was less than 1% in both methods.

A. Ionization cross section differential in ejected-electron energy

The singly differential cross section for ionization as a function of ejected-electron energy is calculated using Eq. (3). Results obtained within the two-electron WP-CCC approach are presented in Fig. 1 (upper panels) in comparison with experimental data [17–21] and other calculations [15,21,25,33]. The results are presented in the laboratory frame. As seen from the figure, the two-electron WP-CCC results of the SDCS in ejection energy agree very well with all the available experimental data at 75, 100, and 300 keV, but only one set of measurements at 150 keV. The lower panels in Fig. 1 show the separate components corresponding to DI and ECC obtained in the two-electron WP-CCC method. The results obtained using the E1E treatment of the helium target are also shown in the lower panels. As we can see, the E1E WP-CCC results are practically similar to the corresponding two-electron ones.

To be more specific, at 75 keV, the two-electron WP-CCC results are in excellent agreement with the experimental data by Schulz *et al.* [21] over the range where the data are available. Noticeably, they also reproduce the slight shoulder present in the experimental data. This feature occurs when the ejected-electron velocity is approximately equal to that of the projectile. At the matching velocity the ejected-electron energy is 40.8 eV, and that is exactly where the shoulder of the SDCS obtained in the two-electron WP-CCC approach is. This is a very satisfying result. The less-accurate E1E WP-CCC calculations are also capable of displaying this subtle feature. Other calculations available at this energy are the BA and BA-PCI results of Schulz *et al.* [21]. The BA-PCI results were originally presented with a scaling factor of 0.5 to compare with the experiment in shape. Figure 1 shows unsclaled results. Though the BA-PCI results overestimate the experimental data in magnitude, they are in better agreement in shape. On the other hand, the simpler BA results are in better agreement with the data in magnitude, however, they do not reproduce the shoulder structure around 40.8 eV.

The situation at 100 keV is somewhat similar. The two-electron WP-CCC results are in excellent agreement with all experimental data [17,18,20,21] over the entire ejected-electron energy range. The BA-PCI results of Schulz *et al.* [21] and FBA results of Manson *et al.* [15] fall below the experimental data of all experiments, though, somewhat surprisingly, agreement improves for the simple hydrogenic FBA approximation [15] for ejected-electron energies larger than 100 eV. Of note is the fact that the present WP-CCC results again exhibit a slight but noticeable shoulder at 54.4 eV ejection energy which is the ejection energy where the velocity of the electron matches that of the projectile. The CTMC results of Schulz *et al.* [21] and Reinhold and Olson [33] also agree with experimental data, particularly at small ejected-electron energies, though these calculations do not display the shoulder structure. The results of Reinhold and Olson [33] begin to slightly underestimate the experimental data and other methods as the ejected-electron energy increases. The classical BE-FF approach of Gryziński [25,26] does not agree with any experimental data at all, having too steep a slope initially and falling below and then flattening to overestimate data at large ejected-electron energies.

At 150 keV, again the present two-electron WP-CCC results exhibit a slight but quite noticeable shoulder at 81.6 eV ejected-electron energy corresponding to the speed of the projectile. Our results agree perfectly with the experimental data of Rudd and Jorgensen [17] over the entire ejected-electron energy range. We also observe reasonably good agreement with the experiment of Schulz *et al.* [21] at the lower emission energies where these measurements were taken.[2] The BA-PCI and CTMC calculations of Schulz *et al.* [21] are in excellent agreement with both experiments [17,21] as well as our results for ejection-energies below 40 eV, though they begin to underestimate the data after this point. These calculations

[2]There is a misprint in Fig. 11 of Ref. [21]. The decade starting with 1×10^{-19} is mislabelled as 3×10^{-19}. We thank Michael Schulz for bringing the misprint to our attention.

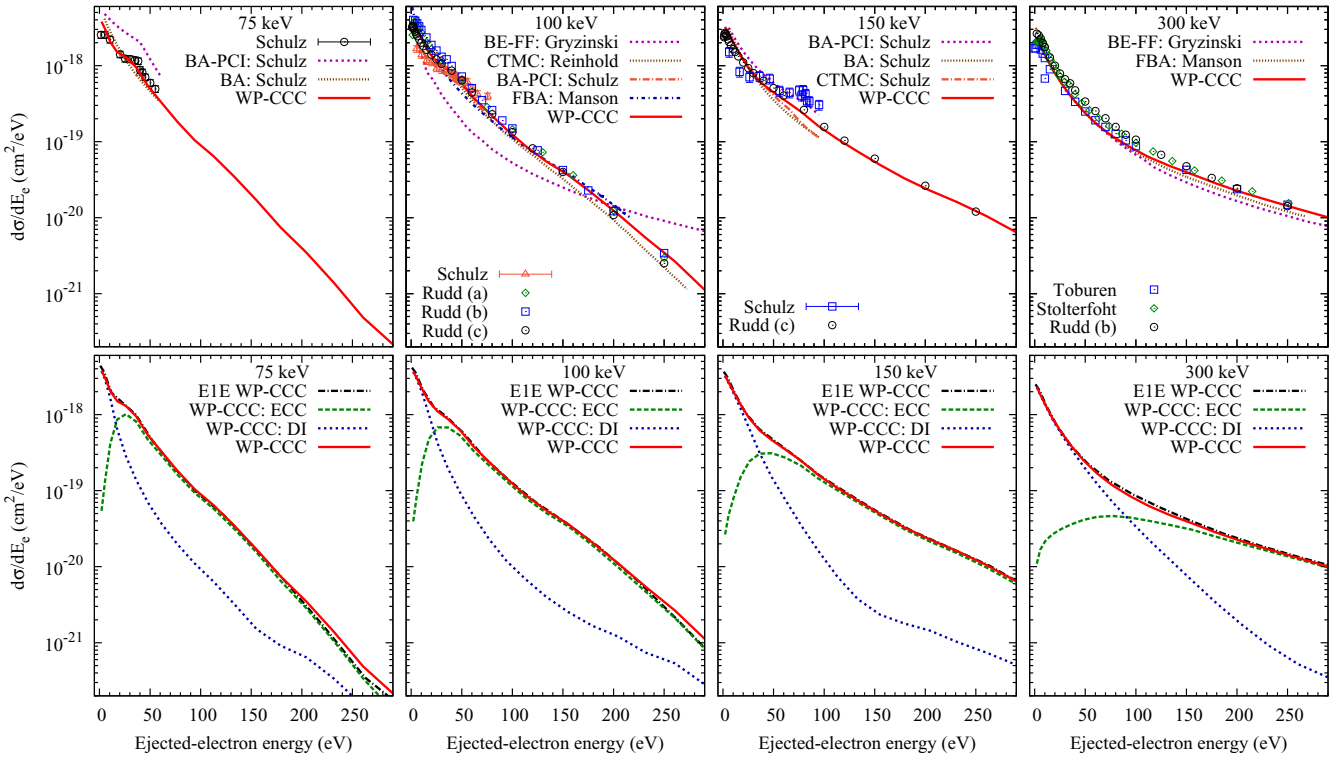

FIG. 1. Singly differential cross section for ionization as a function of ejected-electron energy. Projectile energies are 75, 100, 150, and 300 keV. The upper panels show experimental data by Schulz *et al.* [21], (a) Rudd and Madison [18], (b) Rudd *et al.* [20], (c) Rudd and Jorgensen [17], Manson *et al.* [15] (labeled as Toburen), and Rudd *et al.* [19] (labelled as Stolterfoht) (Note: The raw data labeled in the figure as (a)–(c) Rudd, Toburen and Stolterfoht are taken from Ref. [19]. As described in Ref. [19], the (b,c) Rudd data were recalculated to remove certain experimental error, while the Toburen data came from Manson *et al.* [15] and was averaged to reduce the number of data points. The Stolterfoht data came from multiple sources. See Ref. [19] for details). The lines represent the theoretical results from the present two-electron WP-CCC approach, the BA, BA-PCI and CTMC approaches of Schulz *et al.* [21], the FBA (with the Hartree-Slater type target wave function) by Manson *et al.* [15], the CTMC approach of Reinhold and Olson [33], and the classical BE-FF method of Gryziński [25,26]. The lower panels show the contributions to the SDCS from direct ionization and electron capture into continuum obtained in the two-electron WP-CCC approach. The results of the E1E WP-CCC approach are also shown.

also display a slight shoulder around 81.6 eV ejected-electron energy while the BA does not. The BA-PCI tends to overestimate the experiment of Rudd and Jorgensen [17] and all other theoretical approaches across the energy range presented. However, for ejected-energies greater than 50 eV, the BA-PCI is in good agreement with the Schulz *et al.* [21] experiment. At these energies, this experiment slightly deviates from the other available experimental data [17].

By 300 keV projectile energy, the aforementioned shoulder structure, expected at 163.3 eV, has dissipated completely, a change that is reflected in our results. The two-electron WP-CCC results are in excellent agreement with the experimental data of Rudd *et al.* [20], Toburen [15], and Stolterfoht [19]. Agreement with the results from the hydrogenic FBA [15] and classical BE-FF [25,26] methods is very good for low ejected-electron energies, however, they slightly deviate from the experiment at emission energies greater than 100 eV. For such simple approaches, fairly good agreement is seen with the experimental data as the collision energy becomes sufficiently high. Also noticeable is the significant improvement of the classical BE-FF method in comparison to 100 keV collision energy.

The lower panels in Fig. 1 also show the contributions to the SDCS from direct ionization and electron capture into continuum for the two-electron WP-CCC approach. The components of the SDCS obtained in the E1E WP-CCC approach not shown here are somewhat similar. The effect of electron capture to the continuum changes depending on the ejected-electron energy. It can be seen that at collision energies of 75 and 100 keV, the ECC contribution constitutes most of the net differential cross section everywhere except for a narrow range of small ejected-electron energies. At 150 keV, the ECC component dominates the net cross section at ejected-electron energies above 50 eV. By 300 keV, the low-energy region where the DI component dominates extends to about 80 eV. For low ejected-electron energies, the ECC component is negligible but becomes dominant beyond 80eV, ensuring excellent agreement with the experiment. Thus we can see the importance of including DI and ECC and close coupling between these channels in achieving a realistic picture of the energy-differential ionization process at intermediate energies.

As discussed above, the experimental energy-differential cross sections at projectile energies 75, 100, and 150 keV by Schulz *et al.* [21] show a small shoulder. This physically important feature appears at the ejection energy when the corresponding electron velocity matches the projectile velocity and is reproduced in our calculations. As one can see in

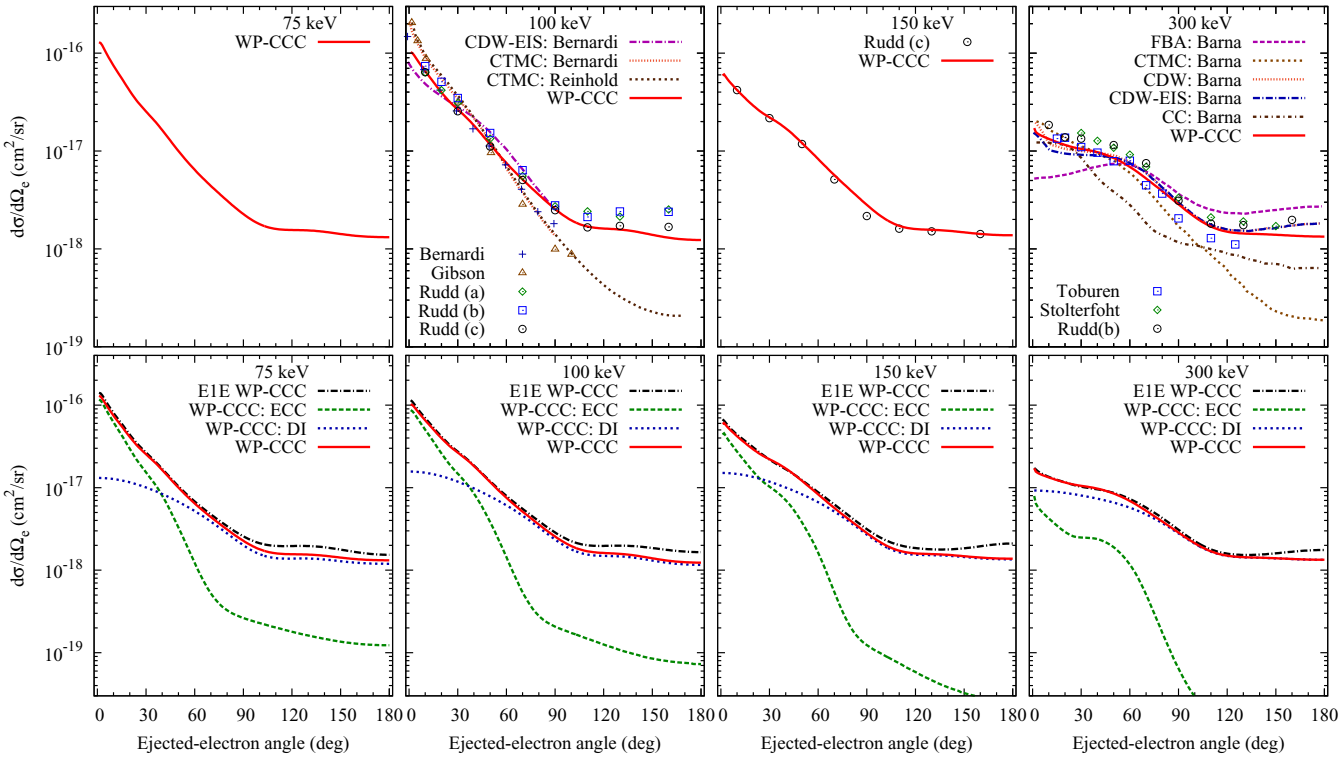

FIG. 2. Singly differential cross section for ionization as a function of ejected-electron angle. Projectile energies are 75, 100, 150, and 300 keV. The upper panels show experimental data by (a) Rudd and Madison [18], (b) Rudd *et al.* [20], (c) Rudd and Jorgensen [17], Toburen [15], Stolterfoht [19], Gibson and Reid [12], and Bernardi *et al.* [11]. The lines represent the theoretical results from the present two-electron WP-CCC approach, the FBA and CDW methods of Barna *et al.* [22], the CDW-EIS methods of Bernardi *et al.* [11] and Barna *et al.* [22], the CTMC methods of Reinhold and Olson [33], Bernardi *et al.* [11] and Barna *et al.* [22], and the CC method of Barna *et al.* [22]. The lower panels show the contributions to the SDCS from direct ionization and electron capture into continuum for the two-electron WP-CCC approach. The results of the E1E WP-CCC approach are also shown.

the lower panels of Fig. 1, the bump appears at the electron energy where the ECC component of the cross section peaks. However, the measurements by the Rudd group [17,18,20] do not show such a feature. This must be due to differences in the experimental methods used by these two groups. The Rudd group measured the doubly differential electron spectra as a function of electron angle and energy. The smallest angle they looked at was 10°. It is well known, however, that at the velocity-matching point the ECC peak in the doubly differential electron spectra as a function of electron angle and energy only occurs in a very narrow angular range around the forward direction, well within 10°. Therefore, in the data by the Rudd group the contributions from ECC are probably significantly underestimated, which could explain the missing bump. On the other hand, the method used by Schulz *et al.* [21] is based on measuring the doubly differential projectile energy loss spectra. It inherently integrates over all electron angles and takes into account the ECC contributions more accurately.

B. Ionization cross section differential in ejected-electron angle

The differential cross section for ionization as a function of the ejected-electron angle is calculated using Eq. (4). The results obtained within the two-electron WP-CCC approach are presented in the upper panels of Fig. 2 in comparison with the experimental data [11,12,17,18,20] as well as other calculations [11,22,33]. Similar to the SDCS as a function of the ejected-electron energy, the results are presented in the laboratory frame. Generally, the ionization cross section obtained using the two-electron WP-CCC method agrees very well with the experimental results, where available. The lower panels in Fig. 2 show the separate components corresponding to DI and ECC obtained in the two-electron WP-CCC method. The results obtained using the E1E treatment of the helium target are also shown in the lower panels. As one can see the later results agree very well with the corresponding two-electron results for the forward angles (angles less than 90°). However, they somewhat deviate for the backward angles.

Let us have a closer look at the results. There are no experimental data at 75 keV. At 100 keV the two-electron WP-CCC results agree well with the experiments of Rudd and Jorgensen [17], Rudd *et al.* [20], and Rudd and Madison [18] over the entire ejected-electron angle range. However, they do not agree with the experiments of Gibson and Reid [12] and Bernardi *et al.* [11]. Our results are lower at small angles, though at the same time they overestimate these experimental data at larger angles. Gibson and Reid [12] suggested that the data of Rudd and Jorgensen [17], Rudd *et al.* [20], and Rudd and Madison [18] were inaccurate due to the influence of electrons reflected by the chamber walls or multiple scattering in the target gas. The CTMC calculations of Reinhold and Olson [33] are in agreement with the Gibson and Reid

[12] experiment, however, they do not conclude that this experiment is more accurate than the others. This is because their CTMC approach neglects the correlation effects between the two electrons. As the WP-CCC method uses a correlated two-electron description of the target, this would suggest that the Rudd and Jorgensen [17], Rudd *et al.* [20], and Rudd and Madison [18] measurements, with which the two-electron WP-CCC results agree, might be more accurate in the entire range of ejected-electron angles. The CDW-EIS method of Bernardi *et al.* [11] extends only to 90°, like the CTMC method of Reinhold and Olson [33], but agrees better with the two-electron WP-CCC results within that region.

The two-electron WP-CCC results at 150 keV are in excellent agreement with the experimental data by Rudd and Jorgensen [17] over the entire range of ejected-electron angles. No other theoretical calculations are available at this collision energy.

Overall good agreement between the two-electron WP-CCC results and the experimental data [15,19,20] is again found at 300 keV. A comparative study of several different methods was performed by Barna *et al.* [22] at this energy. The study included the CTMC, FBA, CDW, CDW-EIS, and one-center CC methods. The FBA results sharply deviate from the experimental data for small angles pointing at the importance of the (missing) Coulomb distortion. The CDW and CDW-EIS results of Barna *et al.* [22] that do include the Coulomb distortion indeed give significantly better agreement with the experiment. However, they deviate from each other, and from the experimental data, for angles less than 30°. Here the CDW results lie above the CDW-EIS ones and are closer to the experimental points. At angles greater than 30° both approaches agree with the experimental data. The CTMC results agree with the experimental data for angles below 90° but then significantly underestimate the data at larger angles. The one-center CC results do not agree with the experimental data. This could be due to the small size of the expansion basis used and not due to the single-center nature of the expansion since our calculations show that adding the second center would give a negligible contribution to the SDCS in emission angle at 300 keV.

Again, the lower panels show the contributions to the SDCS from direct ionization and electron capture into the continuum for the two-electron WP-CCC approach. Our calculations reveal an interesting interplay between direct ionization and electron capture into the continuum in the angular-differential cross section as well. They clearly demonstrate that the ionization cross section differential in the angle of the ejected electron is dominated by electron capture into the continuum for emission into small angles, while emission into large angles is purely due to direct ionization.

C. Ionization cross section differential in scattered-projectile angle

The differential cross section for ionization as a function of the scattered-projectile angle is calculated using Eq. (5). The upper panels in Fig. 3 show the present SDCS obtained using the two-electron WP-CCC method in comparison with experimental data [13,14,16] and other calculations [16,24,34,35]. To be consistent with the angular differential cross sections reported in Paper I, the results are presented in the center-of-mass frame. Experimental results are available only at 300 keV. The present results are in particularly good agreement with the experimental data of Giese and Horsdal [13] and Kristensen and Horsdal-Pedersen [14], however, the measurements of Meng *et al.* [16] substantially deviate from them for scattering angles less than 1 mrad. Consequently, our results underestimate this experiment in this angular region. The eikonal distorted-wave approaches [24] with both the static (DW-S) and Coulombic (DW-C) distortion potentials also lead to good agreement with the experimental data of Giese and Horsdal [13] and Kristensen and Horsdal-Pedersen [14]. The PWBA method by Fukuda *et al.* [24] achieved agreement with these experimental data for small angles, though their cross section falls off steeply to significantly underestimate all the other results for scattering angles greater than 0.6 mrad. The FBA of Salin [34] performed better due to its use of the Hartree-Fock-Slater wave function for the helium target. It is in agreement with our results in the forward direction though overestimates the experiments elsewhere. The dCTMC approach of Meng *et al.* [16] significantly overestimates the experimental data by Giese and Horsdal [13], Kristensen and Horsdal-Pedersen [14], and all other theoretical results over the entire angular range. However, these authors agree with their own measurements below 0.5 mrad. The CTMC method of Schultz and Olson [35] was applied at a proton-impact energy of 100 keV. The resulting cross section appears to have a somewhat different shape to the WP-CCC one. However, there are no experimental data available at this energy to compare with and tell which result is more accurate.

The contributions to the SDCS from direct ionization and electron capture into continuum obtained in the two-electron WP-CCC approach are shown in the lower panels in Fig. 3. One can see that at 75 keV collision energy, electron capture into the continuum dominates in the SDCS as a function of the scattered-projectile angle near the forward direction. However, as the collision energy increases direct ionization gradually becomes the dominant mechanism of ionization. This finding reflects the fact that at 75 keV the cross section for electron capture into all bound states of the projectile atom is significantly large and comparable with the ionisation cross section, but falls sharply as the energy increases and becomes orders-of-magnitude smaller than the ionization cross section at 300 keV (see Paper I).

Finally, we see from the lower panels that the singly differential cross section for ionization as a function of the scattered-projectile angle obtained in the E1E approach is practically similar to the full two-electron one at all considered projectile energies. Thus we can conclude that the SDCS as a function of ejected-electron energy and the SDCS as a function of scattered-projectile angle are less sensitive to the accuracy of the target structure. However, the SDCS as a function of ejected-electron angle requires more accurate correlated description of the target when the electron is emitted into the backward angles.

IV. CONCLUSION

The four-body proton-helium differential scattering problem is investigated using the two-center wave-packet conver-

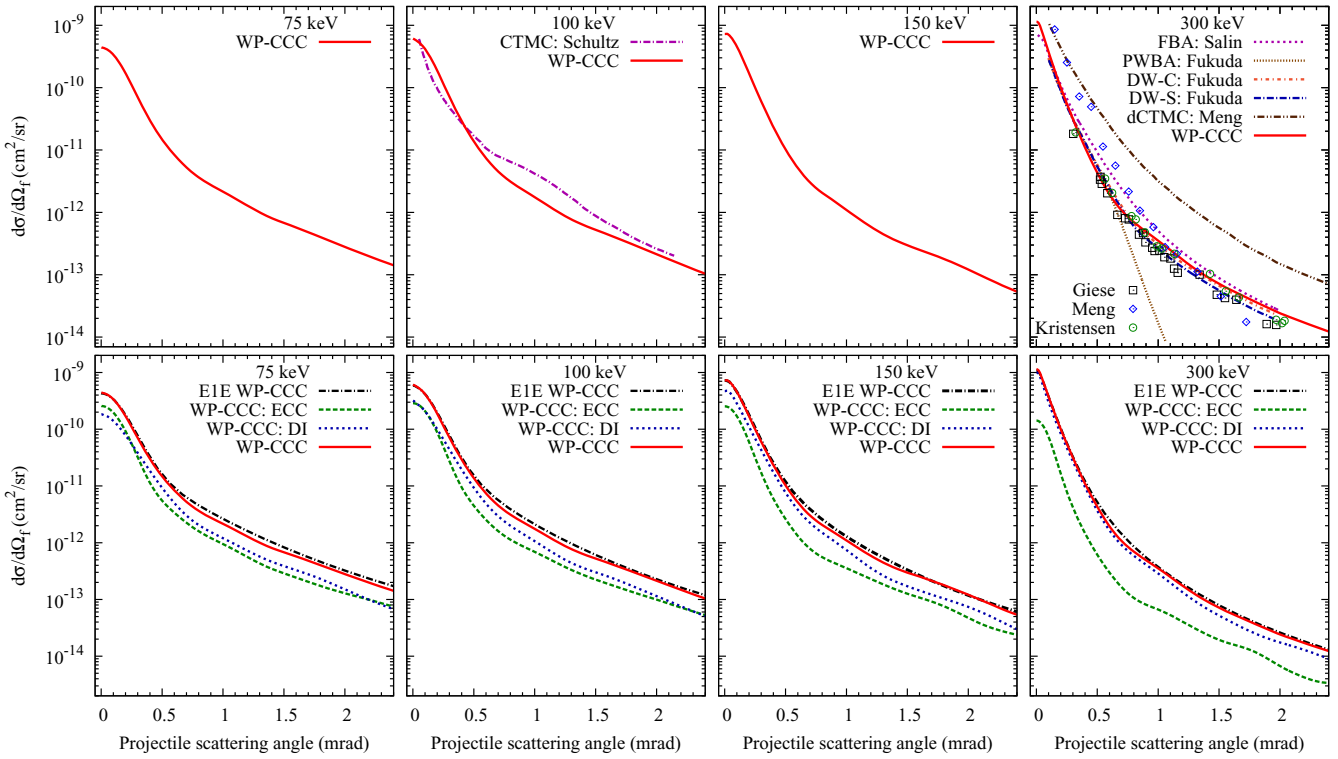

FIG. 3. Singly differential cross section for ionization as a function of scattered-projectile angle. Projectile energies are 75, 100, 150, and 300 keV. The upper panels show experimental data by Giese and Horsdal [13], Kristensen and Horsdal-Pedersen [14], and Meng *et al.* [16]. The lines represent the theoretical results from the present two-electron WP-CCC approach, the FBA of Salin [34], the PWBA by Fukuda *et al.* [24], eikonal distorted-wave methods using a Coulombic (DW-C) and static (DW-S) potentials of Fukuda *et al.* [24], and the CTMC method of Schultz and Olson [35], and the dCTMC approach of Meng *et al.* [16]. The lower panels show the contributions to the SDCS from direct ionization and electron capture into continuum for the two-electron WP-CCC approach. The results of the E1E WP-CCC approach are also shown.

gent close-coupling approach. The approach uses a correlated two-electron wave function for the helium target. The continuum is discretized using wave-packet pseudostates. The singly differential cross sections for ionization as a function of ejected-electron energy, ejected-electron angle, and scattering angle of the projectile in proton-helium collisions at intermediate projectile energies are calculated. The results obtained for the all three types of the singly differential cross section for ionization agree very well with experiments where available. This allows us to conclude that the two-center wave-packet convergent close-coupling approach can provide accurate singly differential cross sections for ionization in proton-helium collisions. Furthermore, our calculations reveal an interesting interplay between direct ionization and electron capture into the continuum in all three differential cross sections. In particular, we demonstrate that the ionization cross section differential in the angle of the ejected electron is dominated by electron capture into the continuum for ejection into small angles, while ejection into large angles is purely due to direct ionization.

We also use a recently developed method that reduces the target to an effective single-electron system. This significantly simplifies the collision problem. A detailed comparison of the results from the two-electron and effective one-electron methods shows that the singly differential cross sections for ionization as a function of the ejected-electron energy and that as a function of the scattered-projectile angle are not very sensitive to electron-electron correlations. However, an accurate correlated treatment of the target somewhat influences the shape of the singly differential cross section as a function of the ejected-electron angle when the electron is emitted into the backward angles. Overall, the results of the two-electron and effective one-electron methods agree with each other quite well. Accordingly, at least for the purpose of calculating the singly differential cross sections for the single ionization of helium, an effective one-electron treatment of the target appears to be adequate. Whether this somewhat unexpected finding holds for more detailed doubly and fully differential cross sections remains to be seen. In any case, the correlated two-electron treatment cannot be disregarded. Obviously, the two-electron processes cannot be described using effective one-electron methods.

In this work we use the WP-CCC approach to calculate all three singly differential cross sections for ionization. In Paper I [45], the method was used to calculate angular differential cross sections for elastic-scattering, target excitation, and electron-capture processes. Comparative analysis provided in these two works demonstrate that the WP-CCC method is a unique approach capable of providing a realistic differential picture of all interdependent and interconnected processes taking place in proton-helium collisions at intermediate energies where coupling between various channels is important.

Thus, one can conclude that the method provides accurate integrated [6] and differential cross sections for all the reaction channels in one calculation. It does this in a unitary fashion by conserving the norm of the total scattering wave function throughout the collision process. The obtained results that are in excellent agreement with the available experimental data position the WP-CCC approach well to investigate the helium ionization process further, in more detail.

We will next turn our attention to doubly and fully differential ionization of helium by ion impact that remains one of the most challenging problems in atomic collision physics. In particular, there is no satisfactory description of the experimental data on the fully differential cross section for the proton-impact ionization of helium at the intermediate projectile energy of 75 keV by Schulz *et al.* [7]. In the scattering plane, the angular dependencies of the fully differential cross section calculated in various methods are generally in good agreement in shape, however, none of them can reproduce the experiment well. Furthermore, in the perpendicular plane there is no agreement between the experiment and various theories for large momentum transfers. The situation is exacerbated by significant deviations between various theoretical results. We hope the WP-CCC approach may shed some light and help better understand the situation.

The single-center version of the WP-CCC method has already been applied to the proton-helium differential ionization [43,44] at sufficiently high energies where electron-capture channels are believed to be negligible. The results of calculations are in excellent agreement with the recent ultrahigh-resolution experiment by Chuluunbaatar *et al.* [59]. However, a small deviation in the position of the binary peak lingers at the smallest considered momentum transfer [44]. We are currently testing if this is due to possible influence of the Thomas double-scattering mechanism that plays an important role in the angular differential cross section for the concurrent electron capture channel [60,61] in the high-energy region.

In closing, we mention that an explanation of the features in the three-dimensional images of the electron emission pattern for the single ionization of helium by the impact of C^{6+} ions at 100 MeV/amu observed by Schulz *et al.* [62] still proves to be a challenging test for theoretical models and remains a controversial topic. We previously investigated the problem using a quantum-mechanical implementation of the CCC method [63] by neglecting the channels representing possible capture of the electron by the projectile. Our results did not support the features reported in Ref. [62]. The two-center WP-CCC method developed here should allow us to investigate possible subtle high-order effects that may require the presence of the second center.

ACKNOWLEDGMENTS

This work was supported by the Australian Research Council. We also acknowledge the resources and services of the Pawsey Supercomputer Centre and the National Computing Infrastructure. C.T.P. acknowledges support through an Australian Government Research Training Program Scholarship. We thank Michael Schulz for reading the manuscript and providing valuable comments.

[1] B. H. Bransden and M. R. C. McDowell, *Charge Exchange and the Theory of Ion-Atom Collisions* (Clarendon, Oxford, 1992).

[2] Dž. Belkić, Review of theories on ionization in fast ion-atom collisions with prospects for applications to hadron therapy, J. Math. Chem. **47**, 1366 (2010).

[3] J. W. Gao, Y. Wu, J. G. Wang, N. Sisourat, and A. Dubois, State-selective electron transfer in $He^+ + He$ collisions at intermediate energies, Phys. Rev. A **97**, 052709 (2018).

[4] Dž. Belkić, I. Bray, and A. Kadyrov, *State-of-the-Art Reviews on Energetic Ion-Atom and Ion-Molecule Collisions* (World Scientific, Singapore, 2019).

[5] M. Baxter and T. Kirchner, Time-dependent density-functional-theory studies of collisions involving he atoms: Extension of an adiabatic correlation-integral model, Phys. Rev. A **93**, 012502 (2016).

[6] S. U. Alladustov, I. B. Abdurakhmanov, A. S. Kadyrov, I. Bray, and K. Bartschat, Wave-packet continuum-discretization approach to proton collisions with helium, Phys. Rev. A **99**, 052706 (2019).

[7] M. Schulz, A. Hasan, N. V. Maydanyuk, M. Foster, B. Took, and D. H. Madison, Kinematically complete experiment on single ionization in 75-kev $p + He$ collisions, Phys. Rev. A **73**, 062704 (2006).

[8] A. Hasan, B. Tooke, M. Zapukhlyak, T. Kirchner, and M. Schulz, Kinematically complete experiment on transfer excitation in intermediate-energy $p + He$ collisions, Phys. Rev. A **74**, 032703 (2006).

[9] M. S. Schöffler, H.-K. Kim, O. Chuluunbaatar, S. Houamer, A. G. Galstyan, J. N. Titze, T. Jahnke, L. P. H. Schmidt, H. Schmidt-Böcking, R. Dörner, Y. V. Popov, and A. A. Bulychev, Transfer excitation reactions in fast proton-helium collisions, Phys. Rev. A **89**, 032707 (2014).

[10] E. C. Beaty, Measurements of the energy and angular distribution of secondary electrons, Radiat. Res. **64**, 70 (1975).

[11] G. C. Bernardi, S. Suárez, P. D. Fainstein, C. R. Garibotti, W. Meckbach, and P. Focke, Two-center effects in electron emission in $^3He^{2+}$-He and H^+-He collisions at intermediate energies, Phys. Rev. A **40**, 6863 (1989).

[12] D. K. Gibson and I. D. Reid, Double differential cross sections for electron ejection from helium by fast protons, J. Phys. B **19**, 3265 (1986).

[13] J. P. Giese and E. Horsdal, Structure in the Differential Charge-State Fractions of He Following Ionization by Fast Protons, Phys. Rev. Lett. **60**, 2018 (1988).

[14] F. G. Kristensen and E. Horsdal-Pedersen, Angular differential measurements of ionization in fast H^+-He collisions, J. Phys. B: At., Mol. Opt. Phys. **23**, 4129 (1990).

[15] S. T. Manson, L. H. Toburen, D. H. Madison, and N. Stolterfoht, Energy and angular distribution of electrons ejected from helium by fast protons and electrons: Theory and experiment, Phys. Rev. A **12**, 60 (1975).

[16] L. Meng, R. E. Olson, R. Dorner, J. Ullrich, and H. Schmidt-Bocking, Differential cross sections for single and double

ionization of helium by protons and antiprotons, J. Phys. B: At., Mol. Opt. Phys. **26**, 3387 (1993).

[17] M. E. Rudd and T. Jorgensen, Energy and angular distribution of electrons ejected from hydrogen and helium gas by protons, Phys. Rev. **131**, 666 (1963).

[18] M. E. Rudd and D. H. Madison, Comparison of experimental and theoretical electron ejection cross sections in helium by proton impact from 5 to 100 keV, Phys. Rev. A **14**, 128 (1976).

[19] M. Rudd, L. Toburen, and N. Stolterfoht, Differential cross sections for ejection of electrons from helium by protons, At. Data Nucl. Data Tables **18**, 413 (1976).

[20] M. E. Rudd, C. A. Sautter, and C. L. Bailey, Energy and angular distributions of electrons ejected from hydrogen and helium by 100- to 300-keV protons, Phys. Rev. **151**, 20 (1966).

[21] M. Schulz, T. Vajnai, A. D. Gaus, W. Htwe, D. H. Madison, and R. E. Olson, Absolute doubly differential single-ionization cross sections in $p+$He collisions, Phys. Rev. A **54**, 2951 (1996).

[22] I. Barna, A. Gagyi-Pálffy, L. Gulyás, K. Tőkési, and J. Burgdörfer, Singly differential electron emission cross sections for ionization of helium by protons, Nucl. Instrum. Methods Phys. Res., Sect. B **233**, 176 (2005).

[23] K. L. Bell, M. W. Freeston, and A. E. Kingston, Differential cross sections for ionization of atomic hydrogen and helium by electron and proton impact, J. Phys. B **3**, 959 (1970).

[24] H. Fukuda, I. Shimamura, L. Végh, and T. Watanabe, Proton angular distributions and highly differential cross sections for ionization of helium by proton impact, Phys. Rev. A **44**, 1565 (1991).

[25] M. Gryziński, Classical theory of electronic and ionic inelastic collisions, Phys. Rev. **115**, 374 (1959).

[26] M. Gryziński, Angular distribution of electrons ejected from helium by protons and the FF atomic model, J. Phys. B **20**, 4741 (1987).

[27] L. Gulyas, P. D. Fainstein, and A. Salin, CDW-EIS theory of ionization by ion impact with Hartree-Fock description of the target, J. Phys. B **28**, 245 (1995).

[28] J. H. Miller, L. H. Toburen, and S. T. Manson, Differential cross sections for ionization of helium, neon, and argon by high-velocity ions, Phys. Rev. A **27**, 1337 (1983).

[29] T. Mukoyama, C.-D. Lin, and W. Fritsch, Calculations of the energy distribution of electrons ejected in ion-atom collisions using pseudostates, Phys. Rev. A **32**, 2490 (1985).

[30] W. J. B. Oldham, Calculations of the energy and angular distribution of electrons ejected from helium by protons, Phys. Rev. **140**, A1477 (1965).

[31] R. E. Olson, T. J. Gay, H. G. Berry, E. B. Hale, and V. D. Irby, Saddle-Point Electrons in Ionizing Ion-Atom Collisions, Phys. Rev. Lett. **59**, 36 (1987).

[32] C. O. Reinhold and C. A. Falcón, Classical ionization and charge-transfer cross sections for $H^+ +$ He and $H^+ + Li^+$ collisions with consideration of model interactions, Phys. Rev. A **33**, 3859 (1986).

[33] C. O. Reinhold and R. E. Olson, Classical two-center effects in ejected-electron spectra from p^+, p^-, and $He^{2+} +$ He collisions at intermediate energies, Phys. Rev. A **39**, 3861 (1989).

[34] A. Salin, Helium ionisation by high-energy ions at a function of impact parameter and projectile scattering angle, J. Phys. B: At., Mol. Opt. Phys. **22**, 3901 (1989).

[35] D. R. Schultz and R. E. Olson, Single-electron–removal processes in collisions of positrons and protons with helium at intermediate velocities, Phys. Rev. A **38**, 1866 (1988).

[36] J. D. Garcia, Ejected electron distributions, Phys. Rev. **177**, 223 (1969).

[37] I. B. Abdurakhmanov, A. S. Kadyrov, S. K. Avazbaev, and I. Bray, Solution of the proton-hydrogen scattering problem using a quantum-mechanical two-center convergent close-coupling method, J. Phys. B **49**, 115203 (2016).

[38] I. B. Abdurakhmanov, A. S. Kadyrov, and I. Bray, Accurate solution of the proton-hydrogen three-body scattering problem, J. Phys. B **49**, 03LT01 (2016).

[39] S. K. Avazbaev, A. S. Kadyrov, I. B. Abdurakhmanov, D. V. Fursa, and I. Bray, Polarization of Lyman-α emission in proton-hydrogen collisions studied using a semiclassical two-center convergent close-coupling approach, Phys. Rev. A **93**, 022710 (2016).

[40] I. B. Abdurakhmanov, A. S. Kadyrov, and I. Bray, Wave-packet continuum-discretization approach to ion-atom collisions: Non-rearrangement scattering, Phys. Rev. A **94**, 022703 (2016).

[41] I. B. Abdurakhmanov, J. J. Bailey, A. S. Kadyrov, and I. Bray, Wave-packet continuum-discretization approach to ion-atom collisions including rearrangement: Application to differential ionization in proton-hydrogen scattering, Phys. Rev. A **97**, 032707 (2018).

[42] C. T. Plowman, K. H. Bain, I. B. Abdurakhmanov, A. S. Kadyrov, and I. Bray, Singly differential cross sections for direct scattering, electron capture, and ionization in proton-hydrogen collisions, Phys. Rev. A **102**, 052810 (2020).

[43] I. B. Abdurakhmanov, A. S. Kadyrov, I. Bray, and K. Bartschat, Wave-packet continuum-discretization approach to single ionization of helium by antiprotons and energetic protons, Phys. Rev. A **96**, 022702 (2017).

[44] I. B. Abdurakhmanov, A. S. Kadyrov, S. U. Alladustov, I. Bray, and K. Bartschat, Fully differential cross sections for single ionization of helium by energetic protons, Phys. Rev. A **100**, 062708 (2019).

[45] K. H. Spicer, C. T. Plowman, I. B. Abdurakhmanov, A. S. Kadyrov, I. Bray, and S. U. Alladustov, Differential study of proton-helium collisions at intermediate energies: Elastic scattering, excitation, and electron capture, Phys. Rev. A **104**, 032818 (2021).

[46] I. B. Abdurakhmanov, C. T. Plowman, K. H. Spicer, I. Bray, and A. S. Kadyrov, Effective single-electron treatment of ion collisions with multielectron targets without using the independent-event model, Phys. Rev. A **104**, 042820 (2021).

[47] I. Abdurakhmanov, O. Erkilic, A. Kadyrov, I. Bray, S. Avazbaev, and A. Mukhamedzhanov, Balmer emission induced by proton impact on atomic hydrogen, J. Phys. B **52**, 105701 (2019).

[48] I. B. Abdurakhmanov, S. U. Alladustov, J. J. Bailey, A. S. Kadyrov, and I. Bray, Proton scattering from excited states of atomic hydrogen, Plasma Phys. Control. Fusion **60**, 095009 (2018).

[49] I. B. Abdurakhmanov, K. Massen-Hane, S. U. Alladustov, J. J. Bailey, A. S. Kadyrov, and I. Bray, Ionization and electron capture in collisions of bare carbon ions with hydrogen, Phys. Rev. A **98**, 062710 (2018).

[50] J. Faulkner, I. Abdurakhmanov, S. U. Alladustov, A. Kadyrov, and I. Bray, Electron capture, excitation and ionization in

$He^{2+} - H$ and $H^+ - He^+$ collisions, Plasma Phys. Control. Fusion **61**, 095005 (2019).

[51] I. B. Abdurakhmanov, C. Plowman, A. S. Kadyrov, I. Bray, and A. M. Mukhamedzhanov, One-center close-coupling approach to two-center rearrangement collisions, J. Phys. B: At. Mol. Opt. Phys. **53**, 145201 (2020).

[52] N. Stolterfoht, D. Schneider, J. Tanis, H. Altevogt, A. Salin, P. D. Fainstein, R. Rivarola, J. P. Grandin, J. N. Scheurer, S. Andriamonje, D. Bertault, and J. F. Chemin, Evidence for two-centre effects in the electron emission from 25 MeV/u Mo^{40+}+He collisions: Theory and experiment, Europhys. Lett. **4**, 899 (1987).

[53] P. D. Fainstein, V. H. Ponce, and R. D. Rivarola, Two-centre effects in ionization by ion impact, J. Phys. B: At., Mol. Opt. Phys. **24**, 3091 (1991).

[54] A. S. Kadyrov, J. J. Bailey, I. Bray, and A. T. Stelbovics, Two-center approach to fully differential positron-impact ionization of hydrogen, Phys. Rev. A **89**, 012706 (2014).

[55] A. S. Kadyrov, I. Bray, A. M. Mukhamedzhanov, and A. T. Stelbovics, Coulomb Breakup Problem, Phys. Rev. Lett. **101**, 230405 (2008).

[56] A. S. Kadyrov, I. Bray, A. M. Mukhamedzhanov, and A. T. Stelbovics, Surface-integral formulation of scattering theory, Ann. Phys. (NY) **324**, 1516 (2009).

[57] F. Herman and S. Skillman, *Atomic Structure Calculations* (Prentice Hall, Englewood Cliffs, NJ, 1963).

[58] R. H. Garvey, C. H. Jackman, and A. E. S. Green, Independent-particle-model potentials for atoms and ions with $36<Z \leqslant 54$ and a modified Thomas-Fermi atomic energy formula, Phys. Rev. A **12**, 1144 (1975).

[59] O. Chuluunbaatar, K. A. Kouzakov, S. A. Zaytsev, A. S. Zaytsev, V. L. Shablov, Y. V. Popov, H. Gassert, M. Waitz, H.-K. Kim, T. Bauer, A. Laucke, C. Müller, J. Voigtsberger, M. Weller, J. Rist, K. Pahl, M. Honig, M. Pitzer, S. Zeller, T. Jahnke *et al.*, Single ionization of helium by fast proton impact in different kinematical regimes, Phys. Rev. A **99**, 062711 (2019).

[60] D. Fischer, M. Gudmundsson, Z. Berényi, N. Haag, H. A. B. Johansson, D. Misra, P. Reinhed, A. Källberg, A. Simonsson, K. Støchkel, H. Cederquist, and H. T. Schmidt, Importance of Thomas single-electron transfer in fast p-He collisions, Phys. Rev. A **81**, 012714 (2010).

[61] H.-K. Kim, M. S. Schöffler, S. Houamer, O. Chuluunbaatar, J. N. Titze, L. P. H. Schmidt, T. Jahnke, H. Schmidt-Böcking, A. Galstyan, Y. V. Popov, and R. Dörner, Electron transfer in fast proton-helium collisions, Phys. Rev. A **85**, 022707 (2012).

[62] M. Schulz, R. Moshammer, D. Fischer, H. Kollmus, D. H. Madison, S. Jones, and J. Ullrich, Three-dimensional imaging of atomic four-body processes, Nature (London) **422**, 48 (2003).

[63] I. B. Abdurakhmanov, I. Bray, D. V. Fursa, A. S. Kadyrov, and A. T. Stelbovics, Fully differential cross section for single ionization in energetic C^{6+}-He collisions, Phys. Rev. A **86**, 034701 (2012).